Fragmentation of rods by cascading cracks: why spaghetti do not break in half

Basile Audoly and Sébastien Neukirch
Laboratoire de Modélisation en Mécanique, CNRS/Université Paris VI, 4 place Jussieu, Paris, France.
(Dated: May 23, 2005)

When thin brittle rods such as dry spaghetti pasta are bent beyond their limit curvature, they often break into more than two pieces, typically three or four. With the aim of understanding these multiple breakings, we study the dynamics of a rod bent just below its limit curvature and suddenly released at one end. We find that the sudden relaxation of the curvature at the newly freed end leads to a burst of flexural waves, whose dynamics are described by a self-similar solution with no adjustable parameters. These flexural waves locally *increase* the curvature in the rod and we argue that this counter-intuitive mechanism is responsible for the fragmentation of brittle rods under bending. A simple experiment supporting the claim is presented.

PACS numbers: 62.20.Mk, 46.50.+a, 46.70.De

The physical process of fragmentation is relevant to several areas of science and technology. Because different physical phenomena are at work during the fragmentation of a solid body, it has mainly been studied from a statistical viewpoint [1–5]. Nevertheless a growing amount of works have included physical considerations: surface energy contributions [6], nucleation and growth properties of the fracture process [7], elastic buckling [8, 9], and stress wave propagation [10]. Usually, in dynamic fragmentation, the abrupt application of fracturing forces (e.g. by an impact) triggers numerous elementary breaking processes, making a statistical study of the fragments sizes possible. This is in contrast to quasi-static fragmentation where a solid is crushed or broken at small applied velocities [11].

Here we consider such a quasi-static experiment whereby a stick of dry spaghetti is bent beyond its limit curvature. Most of the time, the pasta does not break in half but typically into three to ten pieces. This simple and intriguing experiment, which puzzled Feynman himself [12], remains unexplained to date. In this Letter, we explain this multiple failure process and point out a general mechanism of cascading failure in rods: a breaking event induces strong flexural waves which trigger other breakings, leading to an avalanche-like process.

Let us consider a rod which is held at both ends and bent quasi-statically with an increasing, uniform curvature. It breaks at time $t = 0$ when its curvature κ_0 reaches its limit value κ^*: a dynamic crack crosses the weakest section and breaks the rod into two halves. As the rod was initially bent with uniform curvature, the location of this first failure point is that of the strongest defect. We shall not further discuss this initial breaking event, but instead focus on the subsequent dynamics of either half of the rod, for $t > 0$, and show that this dynamics generically leads to new breaking events at later times.

Since we are not interested in the statistics of the initial breaking event, we introduce and analyze throughout this Letter a model problem in which *the release of a rod mimics the initial breaking event*. Both problems indeed obey the same equations but the advantage of the model problem is that the length L of the fragment is known in advance. In the model problem, the rod is initially uniformly bent and at rest. This is achieved by clamping one end and applying a moment M_0 at the other end: M_0 plays the role of the internal moment transmitted across the section that is about to fail, see Fig. 1. At time $t = 0$, this end is suddenly released as the applied moment M_0 is removed instantaneously. The rod no longer is in equilibrium and we study its subsequent dynamics.

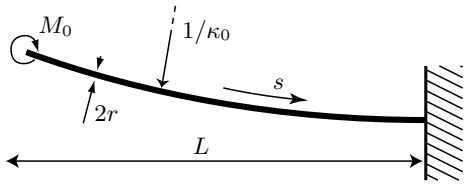

FIG. 1: The dynamics of a rod fragment following the initial breaking event in a brittle rod is modeled by releasing at time $t = 0$ a rod with fixed length L, initial curvature κ_0 and no initial velocity.

The dynamics of thin rods are described by the celebrated Kirchhoff equations [13] which in the limit of small planar oscillations take the form:

$$L^4\,\kappa_{,s^4}(s,t) + T^2\,\kappa_{,t^2}(s,t) = 0, \tag{1}$$

where s is the arclength and a comma in indices denotes a partial derivative. Here, we have introduced a typical time T built from the rod mechanical properties: $T = L^2/\gamma$ where $\gamma = \sqrt{EI/(\rho A)}$, with E the Young's modulus, ρ the mass density, A the area and I the principal moment of inertia of the cross section. For a rod with circular cross section of radius r, $I = \pi r^4/4$ and $\gamma = c\,r/2$, where $c = \sqrt{E/\rho}$ is the sound velocity in the material. Note that T is directly proportional to the period of the fundamental mode of free oscillations of the rod [14], $T_{\text{free}} = 1.79\,T$.

Equation (1) calls for some remarks. First, we base

our presentation on the equations for rods in the limit of small oscillations, and we show that this linear theory captures the essence of the phenomenon (nonlinearities are only considered at the end, in the simulations of Fig. 4). Second, we are only interested in planar configurations of the rod: the rod geometry is parameterized at any time t by a single unknown function of the arclength s, its curvature $\kappa(s,t)$. Although the Kirchhoff equations are classically studied in terms of the transverse displacement $y(s,t)$, we use the curvature as it is the physical quantity connected to the failure of the rod.

On Eq. (1), we impose clamping conditions at $s = L$: $\kappa_{,s^2}(L,t) = 0$, $\kappa_{,s^3}(L,t) = 0$, and free boundary conditions at $s = 0$: $\kappa(0,t) = 0$, $\kappa_{,s}(0,t) = 0$. These four boundary conditions in s associated with the two initial conditions $\kappa(s,0) = \kappa_0$ and $\kappa_{,t}(s,0) = 0$ (uniform curvature κ_0, no initial velocity) warrant, in principle, a unique solution $\kappa(s,t)$ to Eq. (1).

A key remark must be made here, which is at the heart of the rich dynamics of the released rod. These initial and boundary conditions are inconsistent: the curvature $\kappa(0,t)$ at the free end has to be $\kappa_0 \neq 0$ at initial time $t = 0$, while the free end condition requires that it vanishes at any time $t > 0$. This inconsistency can be understood easily: the initial configuration with uniform curvature κ_0 violates the constitutive relation of the rod (the curvature is proportional to the internal moment, even in the dynamic theory of rods) and must therefore vanish near a free end. This is a typical boundary layer situation. The boundary layer, studied in a separate paper [15], restores the small thickness r of the rod into the equations and introduces a small timescale $T_s = r/c$, of order 1 μs for spaghetti, where c is the typical speed of propagation of the transverse dynamic crack. The ratio of this timescale to the 'macroscopic' one reads $T/T_s = 2\,(L/r)^2$. For spaghetti, the aspect ratio is large, $L/r \sim 250$, and so $T/T_s \sim 10^4$. The initial incompatible curvature κ_0 near the edge relaxes over the short timescale T_s. This abrupt relaxation generates a burst of flexural waves which are strong enough to break the rod, as we show later. The separation of time scales allows one to obtain an analytic solution [16] to our problem in the so-called intermediate asymptotic regime

$$T_s \ll t \ll T \tag{2}$$

which we study here. Owing to the obvious scaling $s \sim L\sqrt{t/T}$, we seek a solution of Eq. (1) in the form $\kappa(s,t) = \kappa_0\, u(\xi)$, where the self-similarity variable is $\xi = (s/L)/\sqrt{t/T} = s/\sqrt{(\gamma\, t)}$. Note that we have factored out the initial curvature κ_0, as we use the linear Kirchhoff equations. The boundary conditions for $u(\xi)$ are derived from those for κ: $u(0) = 0$, $u'(0) = 0$ and $u(+\infty) \to 1$. Substituting this self-similar form of $\kappa(s,t)$ into Eq. (1) yields the following equation for the self-similar solution $u(\xi)$:

$$4\, u''''(\xi) + \xi^2\, u''(\xi) + 3\,\xi\, u'(\xi) = 0 \tag{3}$$

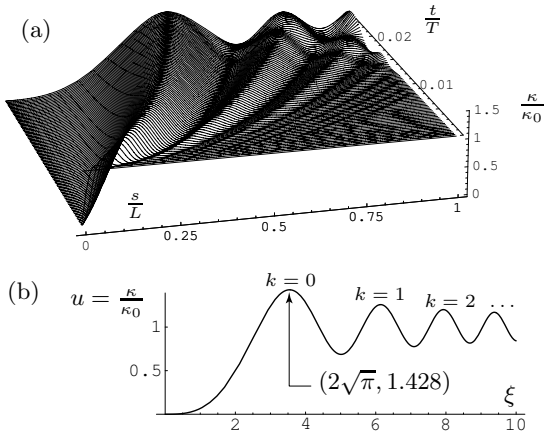

FIG. 2: (a) Numerical solution of the Kirchhoff equation (1) with clamped-free boundary conditions, for a uniform initial curvature κ_0. The curvature at the free end $\kappa(0,t)$ relaxes to zero within the first few time steps (quick relaxation of the incompatible curvature near free end) while it is given in the intermediate regime (2) by the universal self-similar solution (4), shown in (b) as a function of $\xi = s/\sqrt{\gamma\, t}$. At later times, for $t \sim T$, reflections are generated from the clamped end $s = L$.

Imposing that $u(\xi)$ matches the initial condition for large ξ implies that $u''(0) = 0$, as shown with the help of an integral of motion. This last condition, combined with the previous ones, yields a *unique* self-similar solution to Eq. (3):

$$\kappa(s,t) = 2\kappa_0\, S\left(\frac{1}{\sqrt{2\pi}}\,\frac{s}{\sqrt{\gamma\, t}}\right), \tag{4}$$

where we have introduced the Fresnel sine integral, $S(x) = \int_0^x \sin(\frac{\pi}{2}\, y^2) dy$, also arising in diffraction theory. Equation (4) does not describe a progressive wave with constant velocity, $s \sim c\, t$, but instead a self-similar solution $s \sim \sqrt{\gamma\, t}$. This reflects the dispersive nature of Eq. (1).

Bent rods that are suddenly released at one end are all described in the intermediate regime (2) by the same universal solution (4) independently of the material properties, of the details of the initial release or breaking (as long as they take place over a short timescale $T_s \lll T$) and even of the boundary conditions imposed at the other end $s = L$, which have not been used to derive Eq. (4). This universal solution is plotted in Fig. 2 along with a numerical solution of the Kirchhoff equations (1). The latter features, as expected, the self-similar regime for $T_s \ll t \ll T$ in which a burst of flexural waves emitted from the released end $s = 0$ travels along the rod with a square root time dependence. The self-similar solution (4) accurately describes the rod dynamics until reflections on the clamped end $s = L$ take place, for $t \sim T$.

A key property of the self-similar solution (4) is that the curvature $\kappa(s,t)$ is locally significantly *larger* than the initial curvature κ_0. Indeed, for $\xi = 2\sqrt{\pi}$, the self-

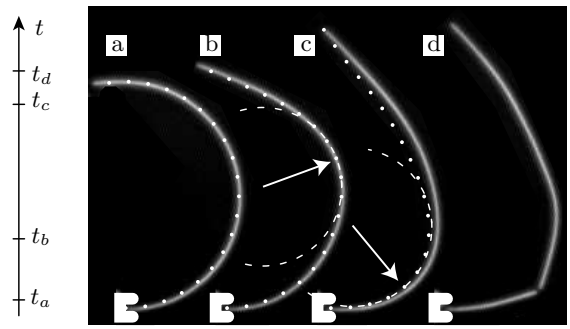

FIG. 3: A dry spaghetti is bent into an arc of circle and suddenly set free, while its lower end remains clamped. Its subsequent dynamics exhibits a local increase of curvature. Selected frames shot with a fast camera at 1000 Hz: (a) release $t_a = 0$, (b) intermediate frame $t_b = 0.0159\,T$, (c) frame just before rupture $t_c = 0.0509\,T$, and (d) after rupture $t_d = 0.0596\,T$. Predictions of the self-similar and numerical simulations based on equation (1) are superimposed, without any adjustable parameters: rod profile (dotted line) and osculating circle (dashed lines) at the point of largest curvature (arrow). Note that the rod breaks at the point of maximal curvature.

similar solution reaches its maximum where the curvature is 1.428 times its initial value κ_0. This coefficient is universal, being twice the maximum of the Fresnel sine integral. It characterizes the maximum of curvature in the intermediate regime (4) (the long time behavior of the curvature is discussed at the end of this Letter). This increase of curvature is indeed observed in the experiment presented in Fig. 3. A Barilla n° 1 dry spaghetti pasta of length $L = 24.1$ cm was clamped and bent into an arc of circle, by an angle $\kappa_0 L = 195°$. Digital photographs were acquired at 1000 frames per second using a fast camera while one end was released. A flexural wave travelling from top (released end) to bottom (clamped end) is clearly visible on the intermediate frames in the form of a local increase of curvature. The predictions of the self-similar solution, namely the point of maximum curvature, $(s/L)/\sqrt{t/T} = 2\sqrt{\pi}$, and the smallest osculating circle with radius $1/(1.428\,\kappa_0)$, are superimposed without any adjustable parameter. The rod profile given by a numerical integration of equation (1) is shown as well [17].

The increase of $\kappa(s,t)$ is rather unexpected. Indeed, one could imagine the motion of the rod to be essentially given by its fundamental mode of oscillation around the straight configuration: $\kappa(s,t) \propto \kappa_0 \cos(2\pi\, t/T_{\rm free})$, where $T_{\rm free} = 1.79\,T$ is the period of free oscillations. This simple picture misleadingly suggests that, after the release of the rod, its curvature remains bounded by its initial value κ_0 at all times, and reaches this value every half-period when the rod is bent the other way around. In fact, the quick initial relaxation of the nonzero curvature $\kappa(0,t)$ at the free end sends a burst of flexural waves, something that is not captured by the fundamental mode only. Such a burst is generated when a brittle rod first breaks. By increasing the curvature locally, this burst triggers secondary breaking events, which ultimately accounts for the multiple failure of brittle rods.

The increase of curvature has thus been described analytically and was confirmed by a direct observation. We now focus on the long time behavior of released rods that break, see Fig. 3 (d). We explain this delayed breaking using the self-similar flexural wave (4), together with its reflections on the clamped end. Analysis of the breaking time and location provides a quantitative check of the theory presented here.

In Fig. 3 (d), the rod ruptured at a distance $s = .76\,L$ from the free end, at a time $t = 6.7$ ms after the release. From the period of free oscillations, we measured $T = 114$ ms directly, hence a dimensionless fracture delay $t/T = 58.5\,10^{-3}$. By repeating the experiment, we found that the failure delay and its location along the rod vary. Failure appears to be extremely sensitive to the initial curvature κ_0 (rods that are closer to their limit curvature tend to break sooner after release, hence closer to the released end) and probably also to the presence of defects. Twenty-five experiments were carried out with various pasta diameters (Barilla n° 1 with $r_1 = .57$ mm and $\gamma_1 = 0.521$ m^2/s; Barilla n° 5 with $r_5 = .84$ mm and $\gamma_5 = 0.735$ m^2/s; Barilla n° 7 with $r_7 = .95$ mm and $\gamma_7 = 0.82$ m^2/s) and initial curvatures (in the range 9.7 m^{-1}–15.3 m^{-1}), with L around 24 cm. All the breaking events collapse onto well-defined regions in a space-time diagram $(s/L, t/T)$, see Fig. 4.

These regions can be calculated as follows. Assuming the rod has no defect, it breaks as soon as its limit curvature κ^* is reached somewhere. The first breaking event after the release must therefore correspond to the first time that $|\kappa(s,t)|$ reaches the value κ^*. This means that breaking occurs necessarily at a point in the plane $(s/L, t/T)$ that is a *record* of curvature since the experiment started: for all s' and all $t' < t$, $|\kappa(s,t)| > |\kappa(s',t')|$. This defines the so-called *absolute* curvature records. Under the opposite assumption that defects are important, κ^* becomes a function of s and rupture is simply expected to take place at a *local* curvature record, that is at a point (s,t) such that $|\kappa(s,t)| > |\kappa(s,t')|$ for all $t' < t$ and same s. Global and local curvature records determined from numerical solution of the full (nonlinear) Kirchhoff equations define a rather narrow region, shown in Fig. 4, onto which the experimental data points indeed collapse with no adjustable parameter.

An analytical prediction for the times of breaking is obtained by considering the interferences between the self-similar wave and its reflection on the clamped end. Constructive interferences lead to strong records of curvature, where breaking events accumulate. The incident wave is characterized by a series of local maxima indexed by an integer $k \geq 0$, see Fig. 2(b), which travel according to $s^2/(4\pi\gamma t) = 2k + 1$: note that the main maximum, $k = 0$, is slower than its precursors, $k \geq 1$. The re-

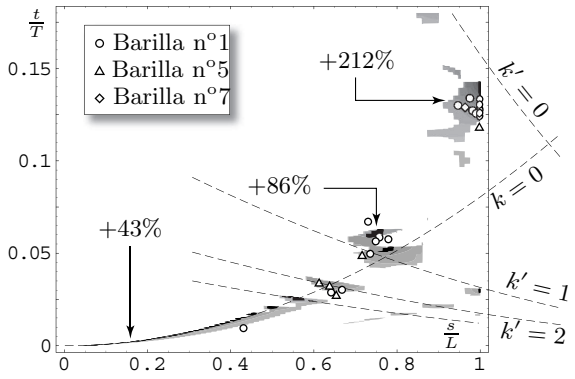

FIG. 4: Space-time diagram, in rescaled coordinates, of the breaking events obtained by repeating the experiment of Fig. 3 (data points) for different pasta radii and initial curvatures κ_0. The time and location of curvature records predicted by numerical simulations of the full (geometrically nonlinear) Kirchhoff equations for $\kappa_0 L = \pi$ are shown in the background, with no adjustable parameters: absolute records (black) and local ones (grey). The breaking event are concentrated on islands which lie approximately at the intersection of the paths (dashed lines) followed by local maxima of the incident and reflected waves (see main text). Percentages show the relative increase of curvature κ/κ_0 at selected points.

flected wave, as constructed by the method of images, has similarly local maxima indexed by $k' \geq 0$ travelling in the opposite direction: $(2L-s)^2/(4\pi\gamma t) = 2k' + 1/2$. Solving for t, the crossing time of the main incident maximum ($k = 0$) and a maximum $k' \geq 0$ in the reflected wave, leads to an analytical prediction of *discrete* breaking times: $t/T = 1/[\pi(1+\sqrt{2k'+1/2})^2]$, that is $t/T = 0.109,\ 0.048,\ 0.033$ for $k' = 0, 1, 2$ respectively. This simple prediction based on the linear theory compares well with both the accumulation of breaking events at rescaled times $t/T \approx 0.13,\ 0.055,\ 0.030$ in the experiments, and with the islands obtained by numerical integration of the full (nonlinear) Kirchhoff equations, see Fig. 4. Note that these rupture delays are considerably shorter than what would be conjectured from a crude analysis, $t/T \sim T_{\rm free}/T = 1.79$.

In the present analysis, we have only considered the first breaking event after release, although multiple failures were commonly observed in experiments [18]. Secondary failure events are most likely described by the same theory, with a shorter timescale T (fragments are shorter) and with the additional difficulty that the initial curvature profile is not uniform. The present physical mechanism for fragmentation of slender elastic bodies, based on flexural waves, leads us to expect specific statistics of fragments sizes. Recall that the maximal curvature increases during the initial boundary layer, $t \sim T_s$, and later reaches a plateau, $\kappa/\kappa_0 = 1.43$. If the initial curvature is sufficiently close to the limit one, very early secondary breaking events should occur and the length scale r should be present in the statistics of fragment size. We have indeed often observed the ejection of tiny rod fragments, with typical size r. However, the fragments were most of the time much larger (with a size comparable to L): the curvature, initially very close to the static limit curvature, was often multiplied by three before rupture was actually initiated. This could be due to the delayed character of the rupture process, which remains to be understood before one can predict the statistics of fragment sizes. The present analysis indeed provides an effective characterization of the breaking times and locations without making use of any specific rupture criterion.

When a bent rod reaches its limit curvature and breaks at a first point, a burst of flexural waves described by a universal self-similar solution is sent through the newly formed fragments, which locally further increases the curvature. The limit curvature is therefore exceeded again at a later time, allowing a cascading failure mechanism to take place. The multiple breaking of spaghetti reflects a peculiar behavior of elastic rods: removing stress can increase strain.

We are grateful to L. Lebon, D. Vallet and K. Liop for their help in setting up the experiments and to E. Villermaux and A. Belmonte for early communication of their work.

[1] N. F. Mott and E. H. Linfoot, Ministry of Supply Report No. AC3348 (1943), unpublished.
[2] D. E. Grady and M. E. Kipp, Journal of Applied Physics **58**, 1210 (1985).
[3] R. Englman, J. Phys: Condens. Matter **3**, 1019 (1991).
[4] L. Oddershede, P. Dimon, and J. Bohr, Physical Review Letters **71**, 3107 (1993).
[5] E. S. C. Ching, S. L. Lui, and K.-Q. Xia, Physica A **287**, 89 (2000).
[6] L. Griffith, Canadian Journal of Research **21**, 57 (1943).
[7] N. F. Mott, Proc. Roy. Soc. London A **189**, 300 (1947).
[8] J. R. Gladden, N. Z. Handzy, A. Belmonte, and E. Villermaux, Phys. Rev. Letters **94**, 035503 (2005).
[9] F. Wittel, F. Kun, H. J. Herrmann, and B. H. Kröplin, Physical Review Letters **93**, 035504 (2004).
[10] D. A. Shockey, D. R. Curran, L. Seaman, J. T. Rosenberg, and C. F. Peterson, Int. J. Rock. Mech. Min. Sci. **11**, 303 (1974).
[11] P. Rosin and E. Rammler, J. Inst. Fuel **7**, 29 (1933).
[12] C. Sykes, *No Ordinary Genius* (W. W. Norton & Company Ltd, 1996), pp. 180-181.
[13] B. D. Coleman, E. H. Dill, M. Lembo, Z. Lu, and I. Tobias, Arch. Rational Mech. Anal. **121**, 339 (1993).
[14] L. D. Landau and E. M. Lifshitz, *Theory of Elasticity*, vol. 7 of *Course of Theoretical Physics* (Pergamon Press, Oxford, 1986), 3rd ed.
[15] B. Audoly and S. Neukirch, in preparation.
[16] G. I. Barenblatt, *Similarity, self-similarity, and intermediate asymptotics* (Consultants Bureau, New York, 1979).
[17] In Fig. 3, the agreement between theory and experiment is further improved with simulations based on the full (geometrically nonlinear) Kirchhoff equations.
[18] See online movies, `http://www.lmm.jussieu.fr/spaghetti`.